Development of Isolated SenseGaN Current Monitoring for Boundary Conduction Mode Control of Power Converters

Mehrdad Biglarbegian, Namwon Kim, Tiefu Zhao and Babak Parkhideh
Electrical and Computer Engineering Department
Energy Production and Infrastructure Center (EPIC)
University of North Carolina at Charlotte
Charlotte, USA
Email: {mbiglarb, bparkhideh}@uncc.edu

***Abstract*—This paper presents the design of the Isolated SenseGaN (Iso-SenseGaN) current sensing technique using Gallium Nitride (GaN) transistors. The isolation technique for the SenseGaN brings an opportunity for integration of sensing element with the power modules, and enables many control schemes in power converters. This could effectively open broader area for smart device monitoring, implementation of current controlling techniques at high frequency, and proper feedback for diagnostics/prognostics developments. In this work, the focus is on the practical challenges for the SenseGaN technique and presenting the inductor-based galvanic isolation. Using the current mirroring method, the authors defined a cursor for detection of the power converter operation mode, i.e., Continuous Conduction Mode (CCM) vs. Boundary Conduction Mode (BCM) in a DC-DC boost and a DC-AC converter a real-time setup.**

***Index Terms*—Boundary conduction mode, boost converter, current-mirroring, inverter, senseGaN, virtual grounding.**

I. INTRODUCTION

Accurate current sensing is among the major design steps toward the Wide Bandgap (WBG) power converters, bringing multiple opportunities such as effective protection, control, and prognostics techniques. Although significant progress has been made in recent years in the development of the advanced current sensors like Hall Effect, Rogowski, and Magneto-resistor sensors, they typically suffer from bandwidth limitations [1]. Traditional resistive-based methods such as Shunt resistor and $R_{ds(on)}$ monitoring, due to their high losses and temperature variation dependency, have some fundamental challenges, especially in high frequency converters [2]. Besides, in power electronics, the current mirroring is commercialized and often known as the SenseFET approach with Si-MOSFET [3]–[6], or has been demonstrated for SiC, and GaN devices integrated with Si MOSFET [7], [8]. Therefore, with significant efforts in increasing the frequency and power in WBG semiconductors (especially GaN), novel sampling techniques are required to provide useful current information for the advanced control strategy [9]. In this paper, the authors target developing a discrete design of current mirroring method with the galvanic isolation to run a DC-DC boost converter and a DC-AC converter in Boundary Conduction Mode (BCM). The active switch current is sensed using the current mirroring technique.

To the best of the authors knowledge, no prior work has been published to sense the active current of power GaN transistors with the galvanic isolation to avoid common mode issues. We called this technique as the Iso-SenseGaN that current monitoring can be effectively used in all common power electronics converters as shown in Fig. 1. The paper is organized as follows: Section II, the methodology of current monitoring with Iso-SenseGaN and the system design by proposing a virtual grounding technique will be provided. Section III, proposes two possible solutions of using Iso-SenseGaN for the BCM control of power converters in the real-time Controller Hardware-In-the-Loop (CHIL), following the Section IV as the conclusion.

II. SYSTEM METHODOLOGY

A. SenseGaN configuration

For circuit-level analysis of current mirroring technique of SenseGaN, one method is to perceive the system as the interconnections of thousands of individual cells in parallel configurations [10]–[13]. The goal is to isolate one of the source connection to use as sensing element, and the measured voltage drop across the resistor can proportionally reflect the current of the active switch. As the power and sense transistors have the common drains and gates, by neglecting the small fraction of a voltage drop across the sensing resistor, the gate-source signal can be assumed the same for both modules. This configuration also provides a unique opportunity to change the width-length ratio (W/L) of the transistor channel, which shows the transistor turn-on resistance [14].

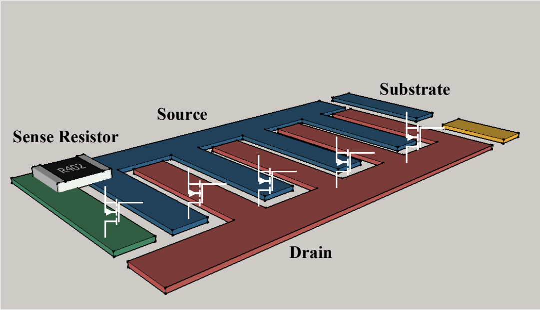

Fig. 1. **Iso-SenseGaN configuration**: Proposing a scheme of Iso-SenseGaN for lateral dies based on available commercial products.

978-1-5386-1180-7/18/$31.00 ©2018 IEEE

Theoretically, this technique does not have any bandwidth limitations; however, to mitigate the effect of temperature dependency and current ratio mismatching of SenseGaN, it is required to optimize sensing resistor shown in Fig. 2. Therefore, based on the proposed technology for compensation of the impedance matching and the virtual grounding, additional circuits should be carefully designed [15].

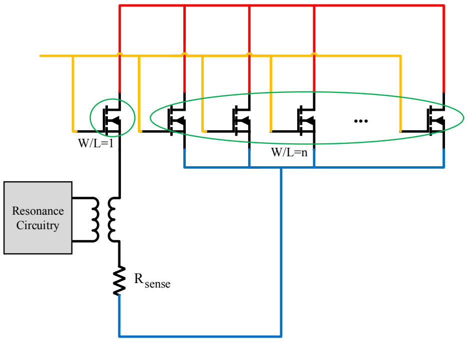

Fig. 2. **Iso-SenseGaN**: The equivalent circuit model of the Iso-SenseGaN for the available lateral GaN.

There are three different methods to provide proper isolation to avoid the voltage common mode issue: a) optical, b) capacitive, and c) electromagnetic isolations. The first method relies on the light intensity proportional to the measured signal coming through the photoconductive element (typically a diode). However, this technique requires at least 0.7V to guarantee the diode is ON. The second method is a proper solution for many systems, but the capacitance characteristics make a longer delay on especially during fast transients. In the electromagnetic method, a pair of conductive coils provides a physical barrier between circuits. The proposed method is the combination of the second and third approaches, where the two small air-core inductors as well as the capacitor-like resonance circuits, and virtual grounding are shown in Fig. 3.

B. SenseGaN Characterization

To analyze the temperature dependency and select proper sense resistance, since both devices will be fabricated with the same technology, the thermal coupling between the transistors will be assumed similarly [16]. Thus, resistance variation of the GaN device at the different temperature is simplified as (1):

$$R_{DS(on)} = R_{DS_{(ON)}}^{25^\circ C} e^{(T-25^\circ C)/k} \tag{1}$$

where, T is the device temperature in Celsius and k is the thermal coefficient of the transistor. The simplified current ratio of the devices is shown in (2):

$$\frac{I_{Q1}}{I_{Q2}} = \frac{R_{DS_{(ON)Q2}}^{25^\circ C}}{R_{DS_{(ON)Q1}}^{25^\circ C}} + \frac{Z_{sense}}{R_{DS_{(ON)Q1}}^{25^\circ C} e^{(T-25^\circ C)/k_{Q1}}} \tag{2}$$

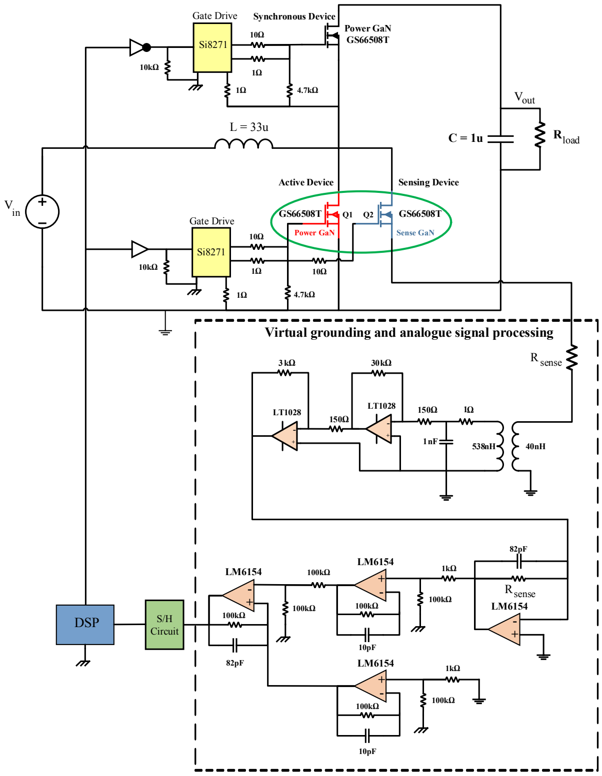

Fig. 3. **Schematic Capture**: a) Schematic of the virtual grounding for Iso-SenseGaN technique with galvanic isolation in a GaN boost converter.

here, Z_{sense} is the total impedance of the Iso-SenseGaN path, and I_{Q1}, I_{Q2} show the current in the power and sense transistors, respectively. Based on (2), to reduce the effect of temperature dependency, the sensing resistor should be very small. However, the drawback is the higher drain current passes through Iso-SenseGaN (Q2), and consequently the high current increases the loss. Therefore, a simple Optimization Function (OF) for each specific design can be run to choose the proper resistance:

$$OF = k_1(P_{con} - \frac{{V_{sw}}^2}{Z_{sense}}) + k_2(1 + Z_{sense}) \tag{3}$$

where, P_{con} is the converter power, V_{sw} is the switching node voltage of the SenseGaN connection, k_1 and k_2 are the weighting factors for objective function, and constant ratio $R_{DS_{(ON)Q2}}^{25^\circ C}/R_{DS_{(ON)Q1}}^{25^\circ C}$ is considered as 1.

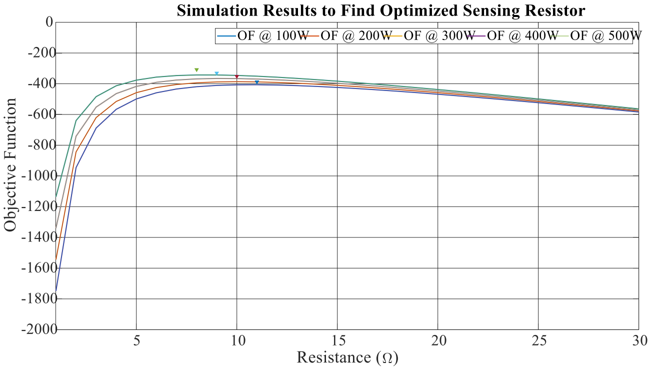

Fig. 4. **Optimization in SenseGaN**: The compromise of higher performance (low resistance) vs. lower loss (high resistance) are analyzed in the OF.

To verify the analysis, a prototype board was built, and the detailed analysis was provided in [15], [17]. The main components are also provided in Table I, and the hardware experimental results of the SenseGaN are shown in Fig. 5.

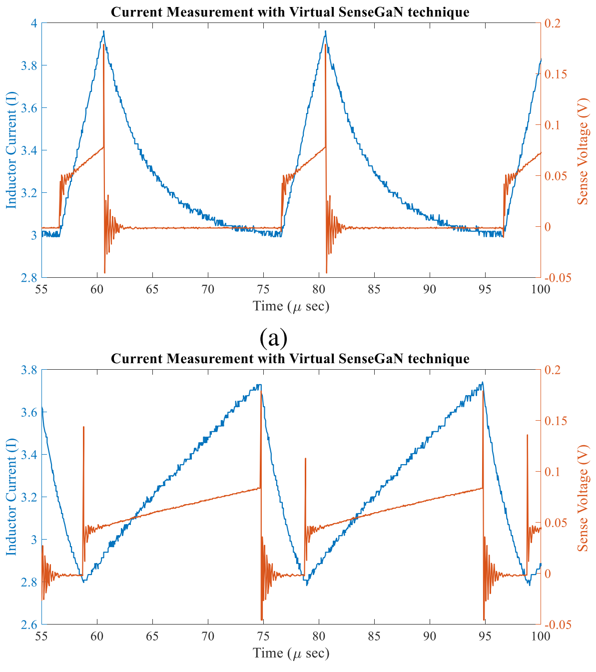

(a)

(b)

Fig. 5. **Experimental Results**: Implementation of SenseGaN prototype under a 150kHz boost power converter a) blue: inductor current measured with an amplifier current gun, orange: current measurement with SenseGaN at 20% duty cycles, and b) blue: inductor current measured with an amplifier current gun, orange: current measurement with SenseGaN at 80% duty cycles.

III. APPLICATION OF ISO-SENSEGAN IN POWER ELECTRONICS CONVERTERS

To show the capability of the Iso-SenseGaN, the BCM control of a DC-DC boost and an inverter are proposed here.

A. *Proposed solution of the BCM in a DC-DC boost converter*

This method initially was introduced in [17], for current monitoring of an active switch in the boost converter. However, the constraints of solution time in microcontroller limit the bandwidth of this technique; Therefore, Iso-SenseGaN can be placed for each device (Q_1), and (Q_2) in the DC-DC boost converter as shown in Fig. 6-a. Once the converter operates at the BCM, the current waveform is characterized as triangle whereas, in the CCM, the current of SenseGaN is considered as trapezoid shown in Fig. 6-b. Having the information of the top and bottom devices, two fast analogue comparators are adjusted with two different thresholds that are placed for each device; the one for the top device indicates the zero current crossing, and for the bottom switch shows the maximum current. Once the trigger signal is received from the high threshold comparator, the bottom device will be turned OFF, and the low threshold comparator turns ON the bottom device, as verified in CHIL test as shown in Fig. 6-c and Fig. 6-d [18].

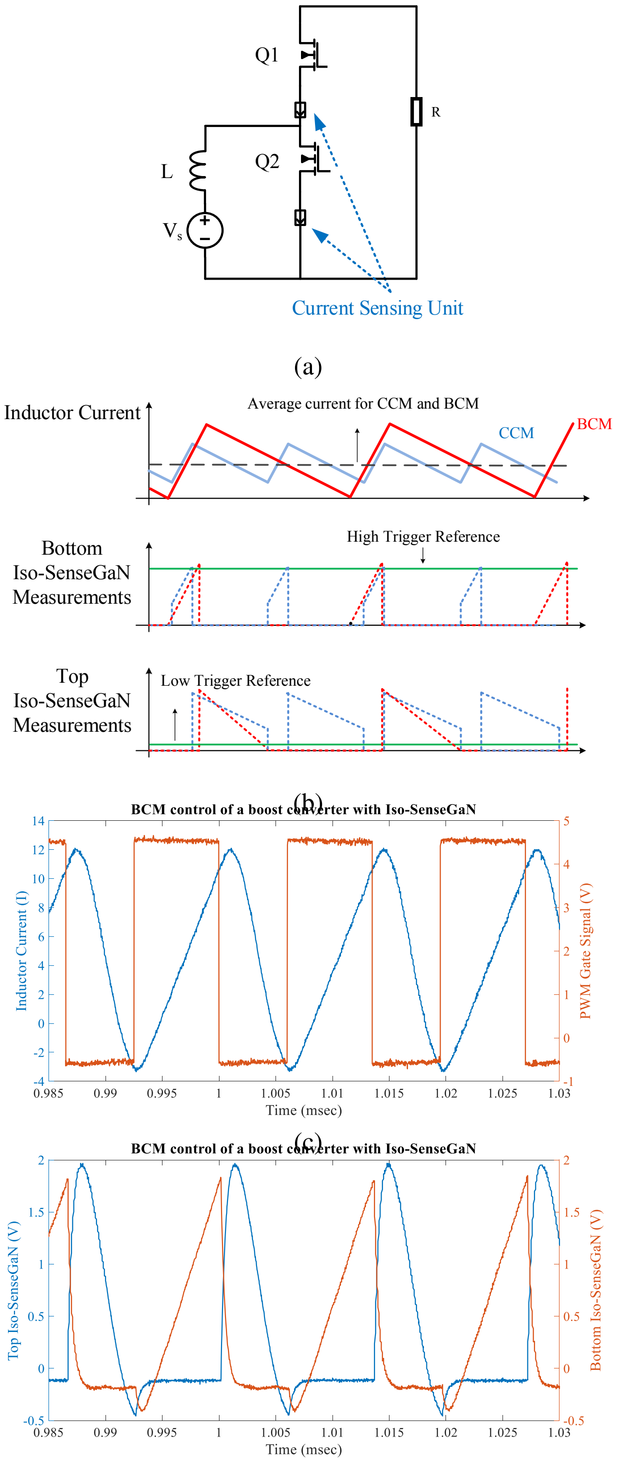

(a)

(b)

(c)

(d)

Fig. 6. **The BCM control of a DC-DC boost converter**: a) the system operation mode at the CCM (blue) and the BCM (red) with the same average current. b) the current monitoring reflected in the Iso-SenseGaN. Two reference trigger signals are considered to turn-on the top and bottom devices consecutive. The closed loop operation of the boost converter operation verified in CHIL test as shown in c) orange: PWM gate signals, blue: inductor current, d) orange: bottom Iso-SenseGaN, blue: top Iso-SenseGaN outputs.

TABLE I
COMPONENTS IN CONVERTER CIRCUIT DESIGN

Item	Manufacturer Part No.	Description
1	GS66516B	GaN transistors
2	SI8271GB-IS	Isolated gate driver
3	PES1-S5-S9-M-TR	Isolated power supply
4	ACM4520-142-2P-T000	Common mode choke filter
5	CD0603-Z3V9	Zener diode
6	LM6154BCM	OpAmp 100MHz Bandwidth
7	C1608X7R1H104K080AA	0.1uF Bypass capacitor
8	C5750X7R2E105K230KA	1uF Bypass capacitor
9	ERJ-3BQF1R0V	1Ω Resistor
10	ERJ-3EKF20R0V	20Ω Resistor
11	ERJ-PA3F4701V	4.7kΩ Resistor
12	ERJ-FC0603E50R0BST1	10kΩ Resistor

B. Proposed solution of the BCM in a DC-AC converter

In this section, the potential of SenseGaN technique is used to control an inverter at the BCM. For each bottom devices, an individual Iso-SenseGaN/SenseGaN will be placed as shown in Fig. 7. Having the information on the bottom devices, two fast analogue comparators adjusted with two small thresholds voltages are considered for each of them, individually. The proposed sensor placement for BCM of the DC-AC converter is shown in Fig. 7.

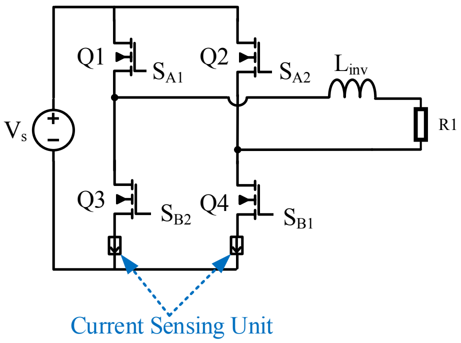

Fig. 7. **SenseGaN for the BCM control of a DC-AC converter**: The proposed architecture for the sensor placement in an inverter.

To understand the inverter operation, the current path is highlighted in Fig. 8. Knowing this, the fundamental switching frequency of the grid is considered as $60Hz$, where two bottom devices (Q_3) and (Q_4) turn on/off in each positive and negative cycles. However, the top switches (Q_1) and (Q_2) operate at the high switching frequency. Using the fast microcontroller (TMS320F28335) for the input signal and the analogue fourth order RC-filter using high-speed operational amplifiers (LM4820) will generate the reference signal. Therefore, the output of the current sensors will be compared with the generated reference current through the high-speed comparators as shown in Fig. 9.

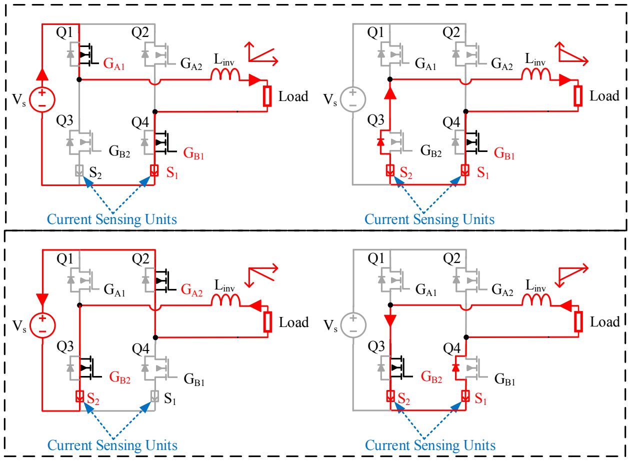

Fig. 8. **Inverter operation**: The system operation for the BCM operation in the inverter, proposed by SenseGaN current mirroring techniques. The current path highlighted with red one shows the four modes of operation.

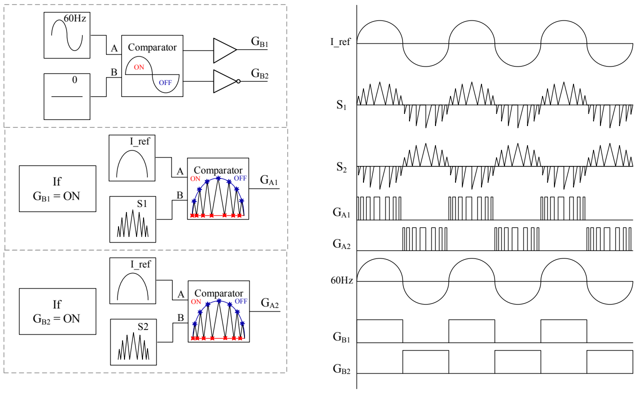

Fig. 9. **Proposed BCM technique**: The analogue circuit logics for PWM generation through SenseGaN and the fundamental frequency of the grid.

The CHIL test result verifies the feasibility of the proposed BCM control strategy in a single-phase inverter as shown in Fig. 10. In the CHIL test, the microcontroller generates the switching signals for the four GaN switches based on the comparison between the current reference and the inductor current captured by the sensing GaN.

Each SenseGaN current unit (S_1 or S_2) is used in each positive or negative cycle of the reference current. In the positive sequence, (Q_4) is turned on continuously. If the active switch current of the (Q_4), (I_{S1}), is zero, corresponding switch (Q_1) is ON. The inductor current is increased based on the inductor voltage and the inductance value. Once the inductor current reaches the current reference, the switch (Q_1) is turned off and the bypass loop with a diode in (Q_3) making the conduction path to decrease the inductor current to zero. Therefore, the BCM operation can be achieved with variable switching frequency based on the inductance, the input and output voltage, and the reference current. In the negative cycle, same procedure occurs with (I_{S2}), (Q_2), and (Q_3).

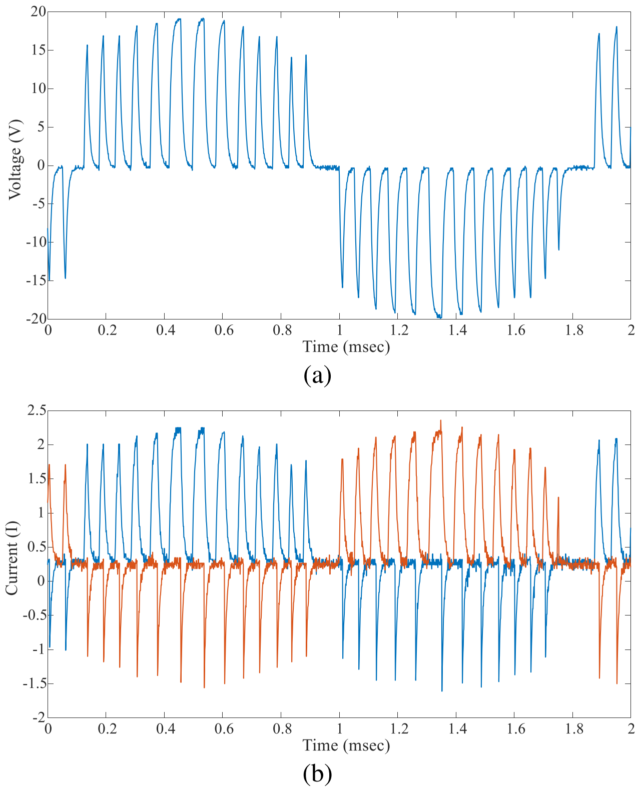

Fig. 10. **SenseGaN for the BCM control of a DC-AC converter**: Two reference trigger signals are considered to turn-on the bottom devices consecutively. The closed loop operation of the DC-AC converter operation is verified in CHIL as shown in a) grid voltage b) top: bottom SenseGaN-1, orange: bottom SenseGaN-2.

IV. Conclusion

This work presented the design and analysis of Iso-SenseGaN technique using power GaN transistors, which can be used in many power electronics topologies. The concept of an integration of power and sense modules in the lateral GaN was introduced. Then, technical challenges like temperature dependency, measurement accuracy, and impedance matching were discussed mathematically. Virtual grounding technique as one of the solutions was proposed and analyzed. To show the potential of the current mirroring technique, two possible solutions for the BCM control of a DC-DC boost converter and an inverter were also verified in CHIL tests.

Acknowledgment

This research was supported by the National Science Foundation under Award No. 1610250. The authors would like to thank the Energy Production and Infrastructure Center (EPIC), and Electrical and Computer Engineering Department at the University of North Carolina at Charlotte.

References

[1] S. J. Nibir, M. Biglarbegian, and B. Parkhideh, “Performance study of magnetic field concentration techniques on Magnetoresistor/Rogowski contactless current sensor,” in *IEEE Sensors, 2016*, 2016, pp. 1–3.

[2] J. Wang, Z. Shen, R. Burgos, and D. Boroyevich, “Design of a high-bandwidth rogowski current sensor for gate-drive shortcircuit protection of 1.7 kV SiC MOSFET power modules,” in *Wide Bandgap Power Devices and Applications (WiPDA), 2015 IEEE 3rd Workshop on*. IEEE, 2015, pp. 104–107.

[3] O. Aiello and F. Fiori, “Current sensing circuit for DC-DC converters based on the miller effect,” in *Applied Electronics (AE), 2013 International Conference*. IEEE, 2013, pp. 1–4.

[4] S. Yuvarajan and L. Wang, “Performance analysis and signal processing in a current sensing power MOSFET (SENSEFET),” in *Industry Applications Society Annual Meeting, 1991., Conference Record of the 1991 IEEE*. IEEE, 1991, pp. 1445–1450.

[5] A. Furukawa, S. Kinouchi, H. Nakatake, Y. Ebiike, Y. Kagawa, N. Miura, Y. Nakao, M. Imaizumi, H. Sumitani, and T. Oomori, “Low on-resistance 1.2 kV 4H-SiC MOSFETs integrated with current sensor,” in *Power Semiconductor Devices and ICs (ISPSD),2011 IEEE 23rd International Symposium on*. IEEE, 2011, pp. 288–291.

[6] ON Semiconductor, “AND8093/D, Current sensing power MOSFETs,” *Semiconductor Components Industries, LLC*, pp. 1–12, 2002.

[7] P. Liu, L. Zhang, A. Q. Huang, S. Guo, and Y. Lei, “High bandwidth current sensing of SiC MOSFET with a Si current mirror,” in *Wide BandGap Power Devices and Applications (WiPDA), 2016 IEEE 4th Workshop on*. IEEE, 2016, pp. 200–203.

[8] Y. Wen, M. Rose, R. Fernandes, R. Van Otten, H. J. Bergveld, and O. Trescases, “A dual-mode driver IC with monolithic negative drive-voltage capability and digital current-mode controller for depletion-mode GaN HEMT,” *IEEE Transactions on Power Electronics*, vol. 32, no. 1, pp. 423–432, 2017.

[9] S. M. Tayebi, N. Kutkut, and I. Batarseh, “Analysis and optimization of BCM peak current mode control techniques for microinverters,” in *Applied Power Electronics Conference and Exposition (APEC), 2017 IEEE*. IEEE, 2017, pp. 2644–2651.

[10] J. L. Vorhaus, “Compound field effect transistor with multi-feed gate and serpentine interconnect,” Sep. 25 2012, US Patent 8,274,121.

[11] GaN System, “How to drive GaN Enhancement mode HEMT,” 2016. [Online]. Available: http://www.gansystems.com/faq-e-mode-hemts.php

[12] A. Lidow, J. Strydom, M. De Rooij, and D. Reusch, *GaN transistors for efficient power conversion*. John Wiley & Sons, 2014.

[13] M. Meneghini, G. Meneghesso, and E. Zanoni, *Power GaN Devices: materials, applications and reliability*. Springer, 2016.

[14] M. Biglarbegian and B. Parkhideh, “Characterization of SenseGaN current-mirroring for power GaN with the virtual grounding in a boost converter,” in *Energy Conversion Congress and Exposition (ECCE), 2017 IEEE*. IEEE, 2017, pp. 5915–5919.

[15] M. Biglarbegian, N. Kim, and B. Parkhideh, “Current monitoring of power GaN transistor,” Jan. 31 2017, Provisional US Application Patent 62452683.

[16] H. Lavrič and R. Fišer, “Lossless current sensing technique on MOSFET RDS(on) with improved accuracy,” *Electronics letters*, vol. 46, no. 5, pp. 370–371, 2010.

[17] M. Biglarbegian, N. Kim, and B. Parkhideh, “Boundary conduction mode control of a boost converter with active switch current-mirroring sensing,” *IEEE Transactions on Power Electronics*, vol. 33, no. 1, pp. 32–36, 2018.

[18] Typhoon HIL, Inc., MA, USA., “Typhoon HIL Real-time Hardware-in-the-Loop (HIL) simulation platform,” Typhoon HIL Control Center Release 2017.3 (2017). [Online]. Available: https://www.typhoon-hil.com/doc/brochures/Typhoon_HIL600_Brochure_downloadable.pdf.